Electronic supplementary information to:

Harvesting the photoexcited holes on a photocatalytic proton reduction metal-organic framework

J. G. Santaclara,[a] A. I. Olivos-Suarez,[a] I. du Fossé,[a] A. Houtepen,[b] J. Hunger,[c] F. Kapteijn,[a] J. Gascon,[a] and M. A. van der Veen*[a]

*M.A.vanderVeen@tudelft.nl

[a] Catalysis Engineering, Department of Chemical Engineering, Delft University of Technology, van der Maasweg 9, 2629 HZ, Delft, The Netherlands.

[b] Optoelectronic Materials, Department of Chemical Engineering Delft University of Technology, van der Maasweg 9, 2629 HZ, Delft, The Netherlands.

[c] Max Planck Institute for Polymer Research, Ackermannweg 10, 55128 Mainz, Germany

Contents

1. Textual properties

N_2-physisorption experiments were carried out at 77 K in a TriStar II unit gas adsorption analyser (Micromeritics). Prior to the measurements the samples were degassed at 423 K under vacuum for 16 h. The BET areas were calculated using intervals allowing positive BET constants.[1] The total pore volumes were calculated at 0.9 relative pressure.

Table S1. Textural properties of the MOFs employed in this work.

MOF	S_{BET} / $m^2\ g^{-1}$	V_p / $cm^3\ g^{-1}$
NH_2-MIL-125(Ti)	1422	0.58

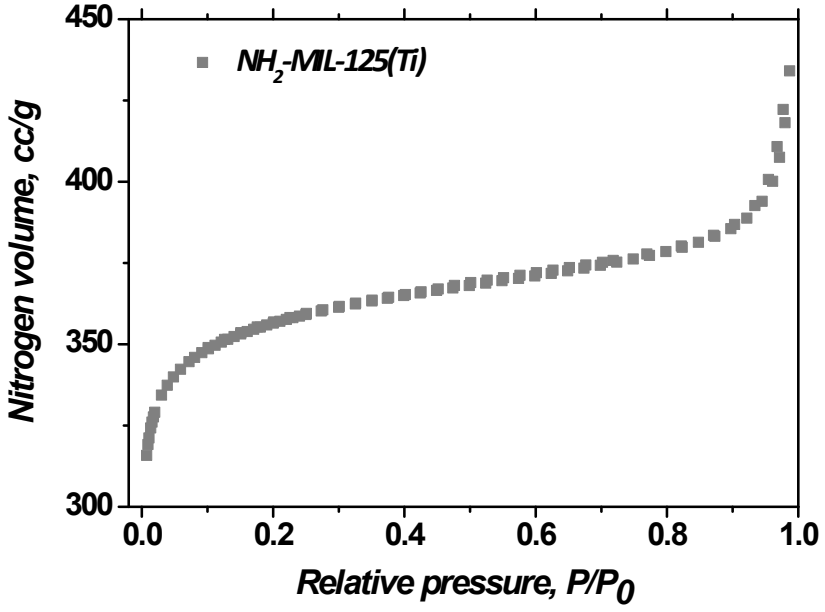

Figure S1. Nitrogen physisorption isotherms at 77 K for NH_2-MIL-125(Ti).

2. Powder X-Ray diffraction

Powder X-Ray diffraction patterns were recorded using a Bruker-AXS D5005 with Co-*Kα* radiation.

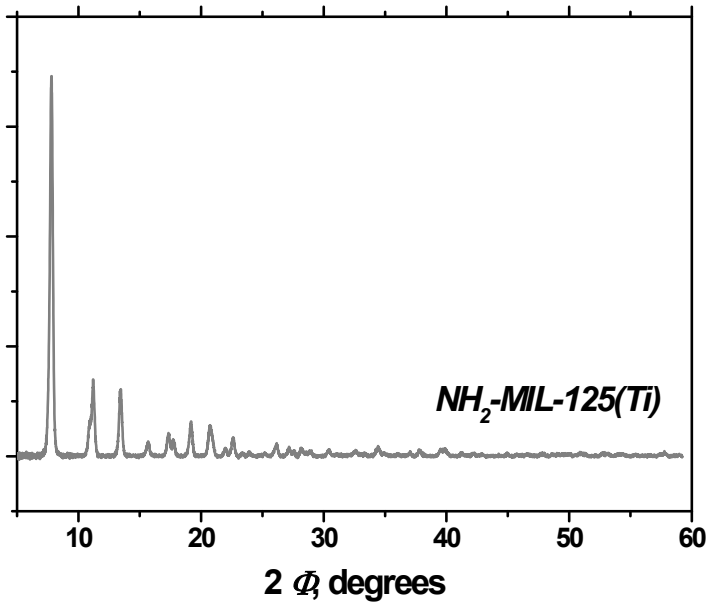

Figure S2. Powder X-Ray diffraction pattern of NH_2-MIL-125(Ti).

3. Thermo Gravimetric Analysis (TGA)

Thermogravimetric analysis (TGA) was performed on a Mettler Toledo TGA/SDTA851e thermobalance, where 10 mg of sample was screened for the change in its mass while being heated from 298 to 873 K at a heating rate of 10 K min^{-1} under 60 cm^3 STP min^{-1} of air flow.

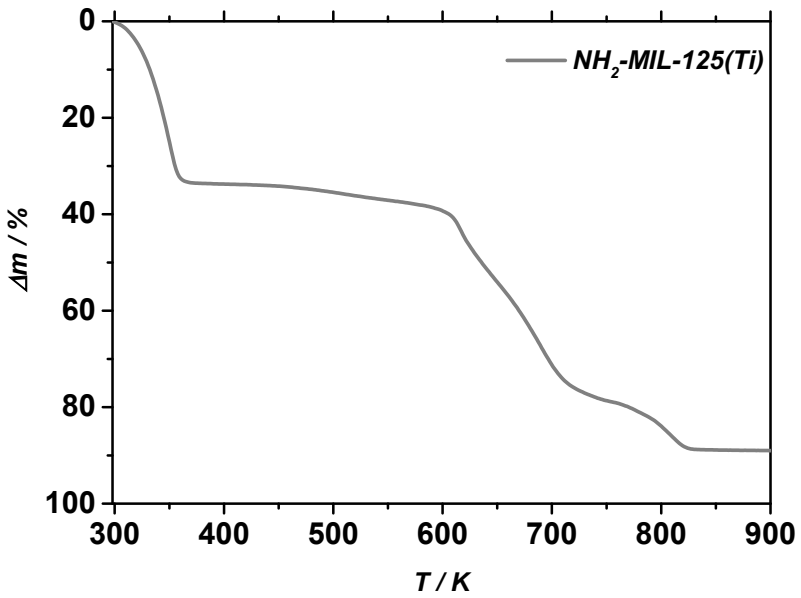

Figure S3. TGA pattern of NH_2-MIL-125(Ti). The sample was heated under air flow at a heating rate of 10 K min^{-1}.

4. Electron donor occlusion

Quantification for the amount of occluded molecules 1, 2, and 3 prepared in acetonitrile

NMR quantification. An internal standard method is used to determine concentration on the liquid and determine the total amount of molecule that is not adsorbed. To adsorb the molecules in the pore we add ~0.7 ml of acetonitrile-d3 the desired amount of molecule and MOF. The resulting suspension is sonicated during 30 minutes and centrifuged to recover the supernatant. An aliquot of 0.5 ml is taken and a nmr standards is added (Maleic acid –d2 for TEA and TEMPO and $DMSO_2$, Aldrich TraceCERT for the pyrazol). The final solution is then measured by ^{1}H-NMR spectroscopy in an Agilent-400 MR DD2 NMR spectrometer. For trimethylamine the signal at δ=1.24 ppm, t 9H was integrated together with that of maleic acid (δ=6.36 ppm, 2H) and the concentration of the amine was directly correlated to that of the standard. For the pyrazole the signal at δ=7.75 ppm, d 1H and δ=7.68 ppm, dd 1H arising from the pyrazole were integrated together and directly correlated to that of DMSO2 (δ=2.91 ppm, 6 H). For TEMPO the signals at δ=1.35 and 1.39 ppm arising from the 4 methyl groups, s 12H were integrated and correlated to that of maleic acid (δ=6.36 ppm, 2H). TMS was used for referencing the spectra.[2]

The concentration of molecules in the composite obtained by NMR, and the corresponding average number of molecules per cage in the MOF, are given in Table 2:

Table S2. Quantification of molecules in the composites by NMR.

Molecule	*mmol /g MOF*	*Molecules/cage*
1	0.005	2
2	0.002	1
3	0.013	6

Quantification for the amount of occluded molecule 3 prepared in water

For **3,** in contrast to UV-VIS transparent **1** and **2**, the quantification can also be done by the more accessible UV-VIS absorption spectroscopy..

50 mg MOF was dispersed in an aqueous solution that contains the electron donor (0.024 M, 14 mL) and sonicated for 30 min. After filtration, the amount of **3** in the liquid was determined by UV-VIS spectroscopy, and by subtracting it from the initial amount of **3** added, the concentration of **3** in the composite was determined.

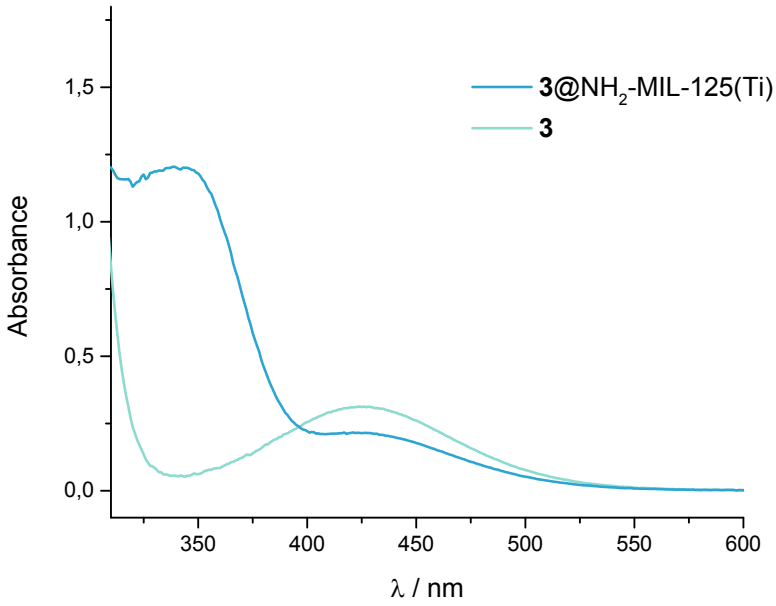

Figure S4. UV-VIS absorption spectra of **3** (maximum absorption at 426 nm) and composite **3**@NH_2-MIL-125(Ti) in water. From the difference between both spectra at 426 nm the amount of **3** occluded in the pores of the MOF was determined.

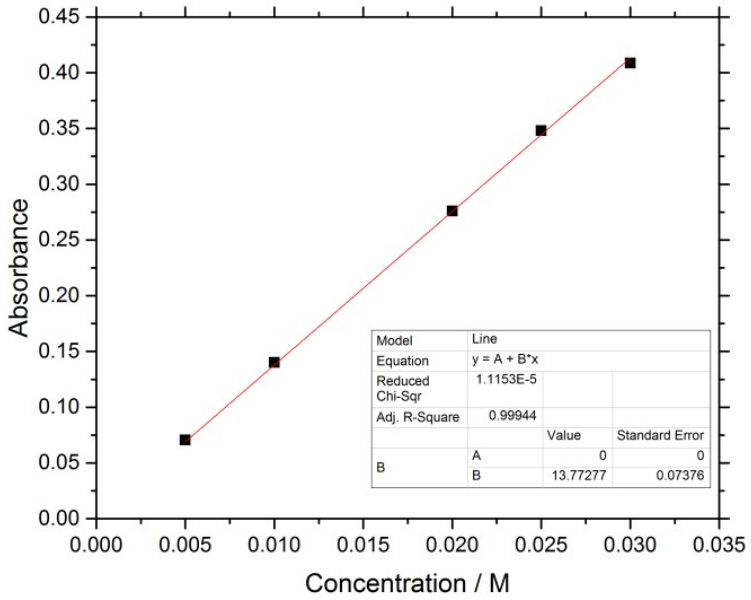

Figure S5. Calibration curve of **3** in water. The formula of the linear fit through the origin, y=13.773x, was used to calculate concentrations from the measured absorbance. This relation, along with its coefficient of determination can be found in the lower right corner.

By this quantification method, we obtained 0.0022 mmol/g_{MOF}, corresponding to one molecule **2** per cage.

5. Photoluminescence

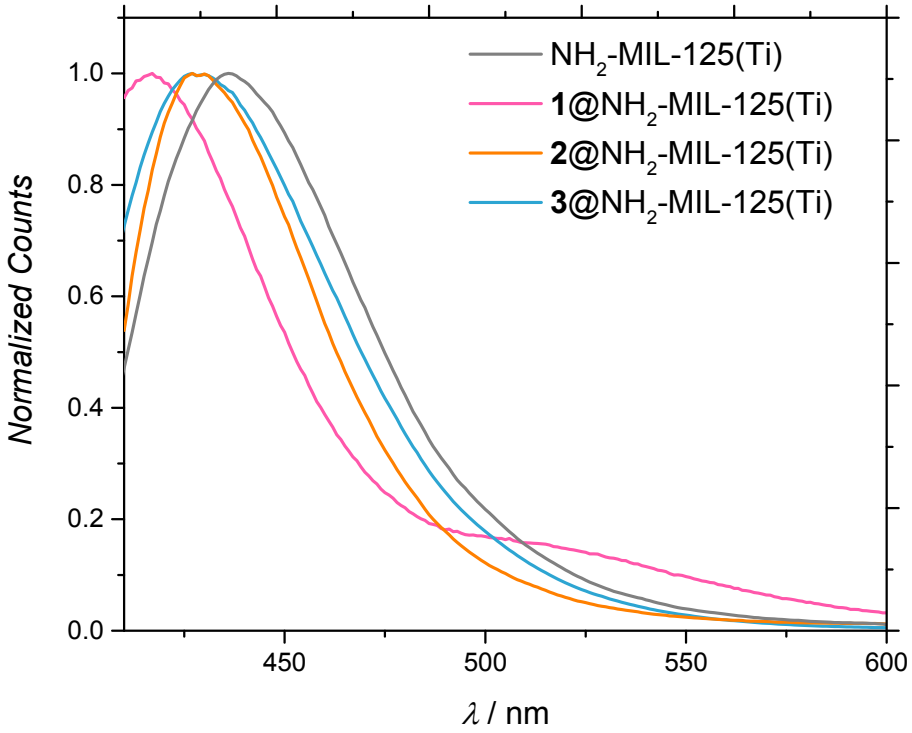

Figure S6. Photoluminescence spectra of NH_2-MIL-125(Ti) in water (*grey*), **1**@NH_2-MIL-125(Ti) in acetonitrile (*pink*), **2**@NH_2-MIL-125(Ti) in DMF (*orange*) and **3**@NH_2-MIL-125(Ti) in water (*blue*). The suspensions of NH_2-MIL-125(Ti) and **3**@NH_2-MIL-125(Ti) in water were excited by a 360 nm laser, **1**@NH_2-MIL-125(Ti) in acetonitrile at 370 nm and **2**@NH_2-MIL-125(Ti) in DMF at 400 nm for a better quality of the data.

6. Time resolved photoluminescence

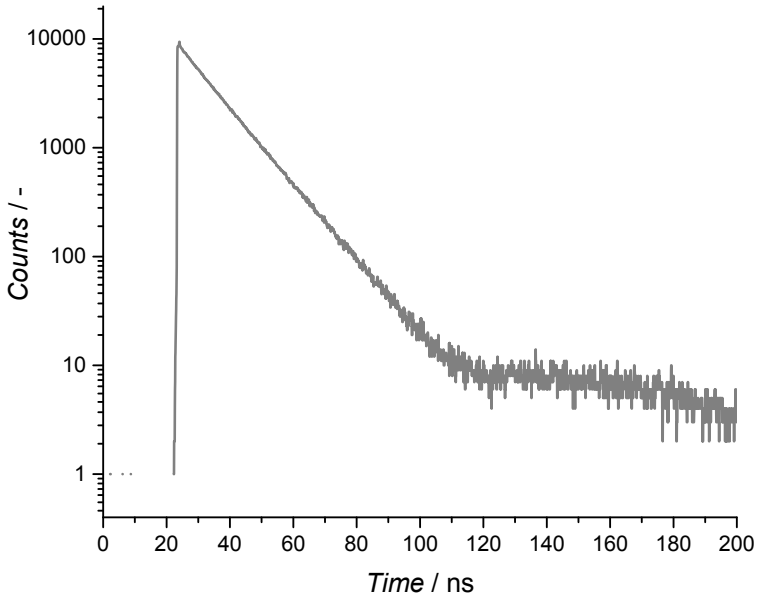

Figure S7. Time resolved photoluminescence spectra of NH_2-MIL-125(Ti) in DMF.

The photoluminescence decay was also investigated for NH_2-MIL-125(Ti) in DMF (exponential decay 12 ns), and previously reported for the solid and the suspension in acetonitrile (characteristic decay times were 11.3 ns and 16.5 ns, respectively)[3]

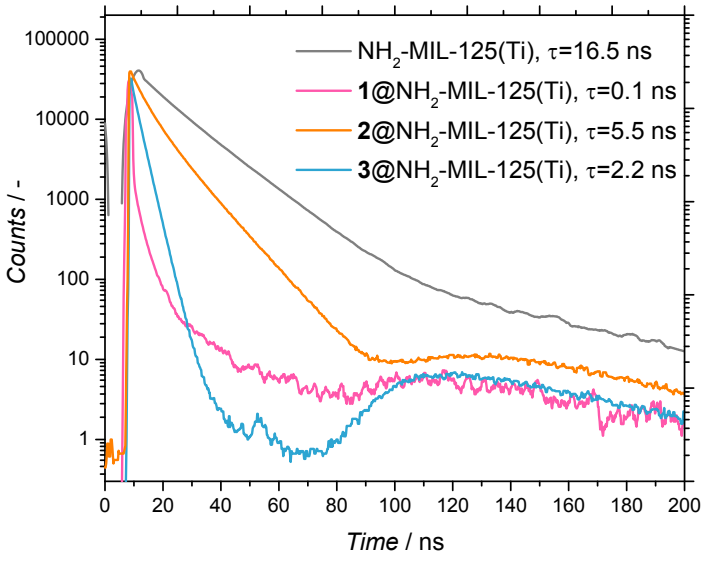

Figure S8. Time resolved photoluminescence spectra of NH_2-MIL-125(Ti) and composites in acetonitrile.

7. Vis pump-Vis probe spectroscopy

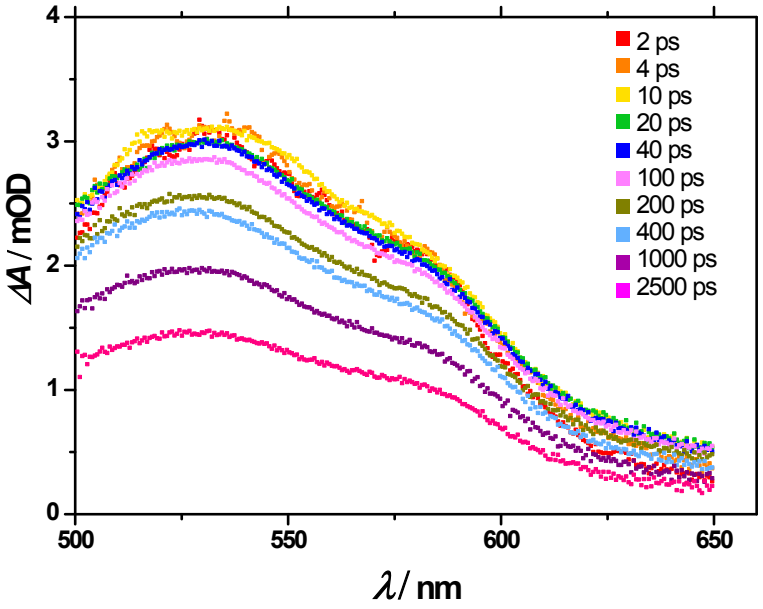

Figure S9. Differential transient absorption spectra for a suspension of NH_2-MIL-125(Ti) in DMF upon excitation at 400 nm

In the case of **2**@NH_2-MIL-125(Ti), charge transfer does not appear to happen using acetonitrile as solventc(Figure S13), obtaining very similar decay dynamics as using the unloaded MOF.[4]

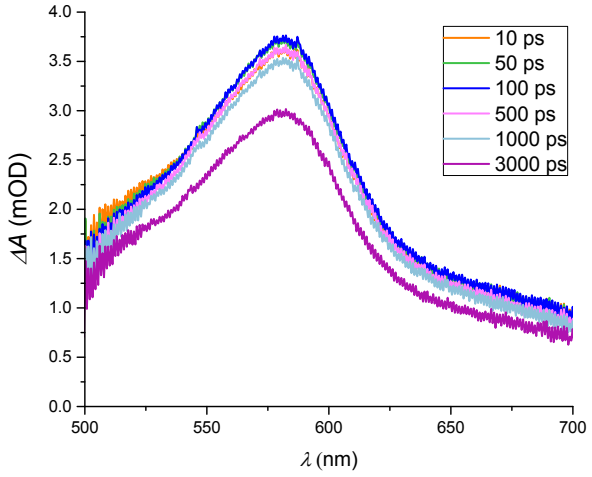

Figure S10. Differential transient absorption spectra for a suspension of **2**@NH_2-MIL-125(Ti) in acetonitrile upon excitation at 400 nm

For composite **3**@NH_2-MIL-125(Ti), charge transfer in acetonitrile occurs in a less efficient manner: the signal attributed to the photogenerated holes decays much faster than in the MOF. Again, we see the fast decay of the signal assigned to the electron on the Ti^{+3}, showing reversible electron transfer (as it was observed in water).

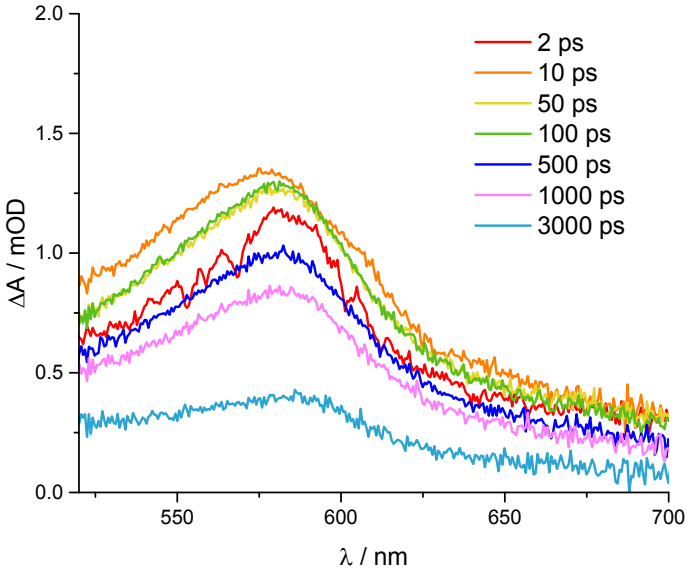

Figure S11. Differential transient absorption spectra for a suspension of **3**@NH_2-MIL-125(Ti) in acetonitrile upon excitation at 400 nm

The decays have been calculated by the equation of exponential decays: $N(t)=N_0\, e^{-\tau t}$

8. Steady state IR spectra

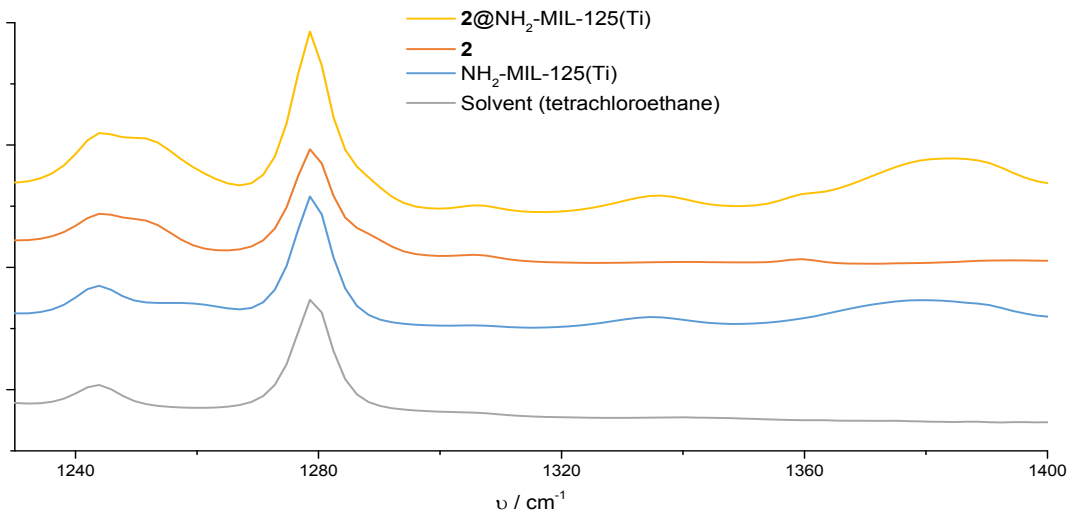

Figure S12. mid-IR spectra for a suspension of **2**@NH_2-MIL-125(Ti) in tetrachloroethane

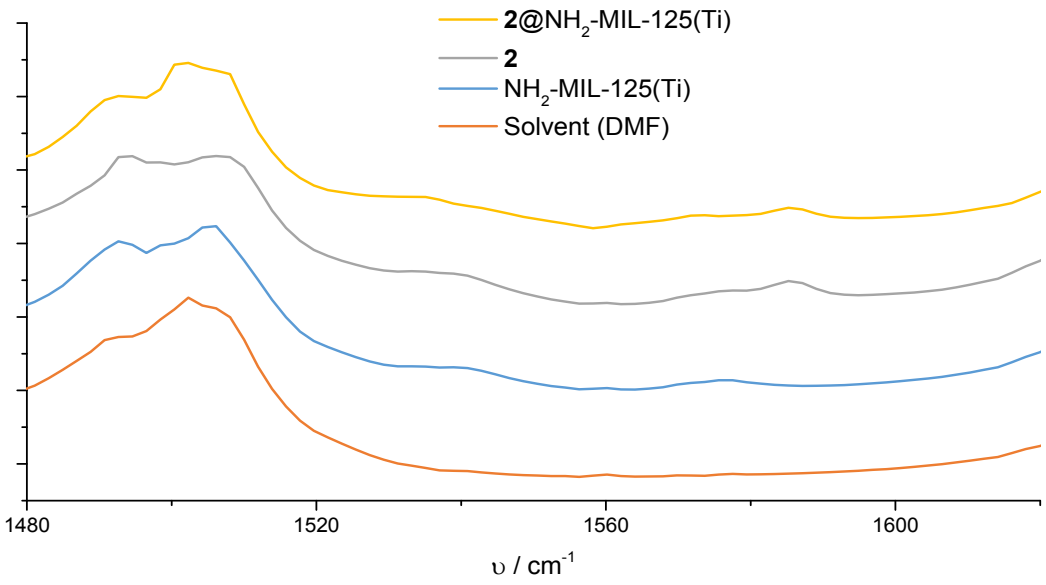

Figure S13. mid-IR spectra for a suspension of **2**@NH_2-MIL-125(Ti) in DMF

9. Vis pump-mid-IR probe spectroscopy

In Figure S14 very different dynamics from the decay of solely the MOF[5] gradually appear. The new spectral features appear with symilar dynamics than Figure 6c (described in the main paper), probably due to the weakened and strengthen of bonds upon charge transfer.

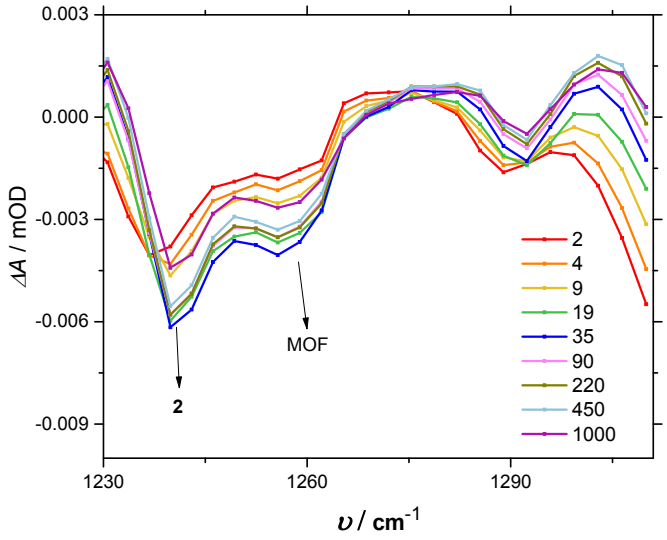

Figure S14. Differential transient absorption mid-IR spectra for a suspension of **2**@NH_2-MIL-125(Ti) in tetrachloroethane upon excitation at 400 nm (range 1210-1310 cm^{-1}).

According to the ground state spectrum of the MOF in our previous publication (J.G. Santaclara et al. ChemSusChem 2016, 9, 388), the 1260 cm^{-1} ground state bleach vibration visible in Figure S14 (also visible in the ground state spectrum of the MOF in figure S12) is assigned to the C-N stretch vibration of the MOF. Both **2** and MOF absorb 1240 cm^{-1} light (see figure S12). Our previous mid-IR pump probe data on solely the MOF (J.G. Santaclara et al. ChemSusChem 2016, 9, 388) show a ground state bleach at 1260 cm^{-1}, but not at 1240 cm^{-1}. This makes it more likely that the observed 1240 cm^{-1} band is related to **2**, or at least due to interaction between the MOF and **2**.

10. Vis pump-Vis probe spectroscopy NH_2-MIL-125(Ti) in DMF

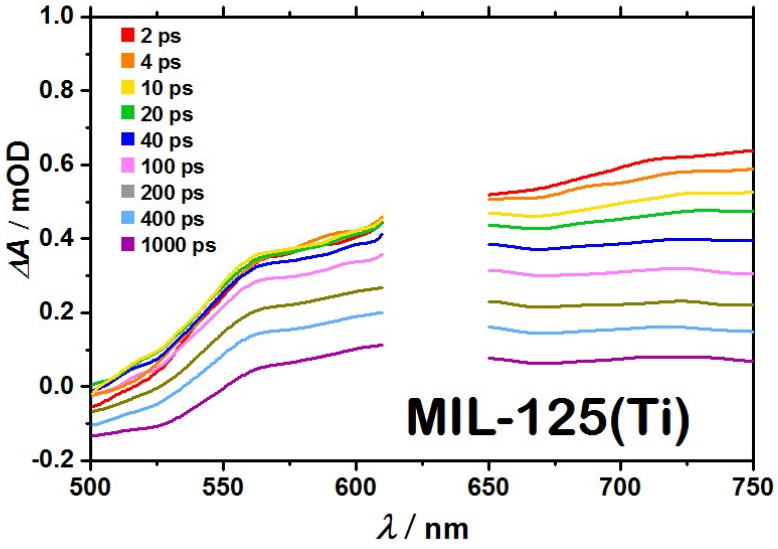

Figure S15. Differential transient absorption spectra for a suspension of MIL-125(Ti) in water upon excitation at 315 nm. The remnant of the 630 nm light used to generate 315 nm light via second-harmonic generation in the pump beam results on a signal between 610-650 nm that overwhelms transient spectra, hence this part of the spectra is omitted.

11. UV/VIS spectroscopy

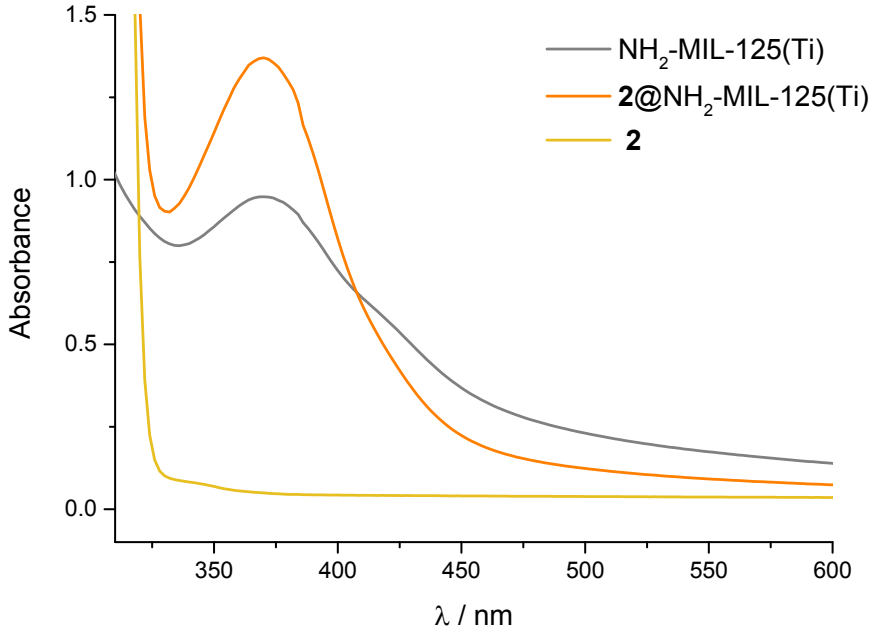

Figure S16. UV/VIS spectra of NH_2-MIL-125(Ti) (*grey*), **2**@NH_2-MIL-125(Ti) (orange) and **2** (yellow) in DMF.

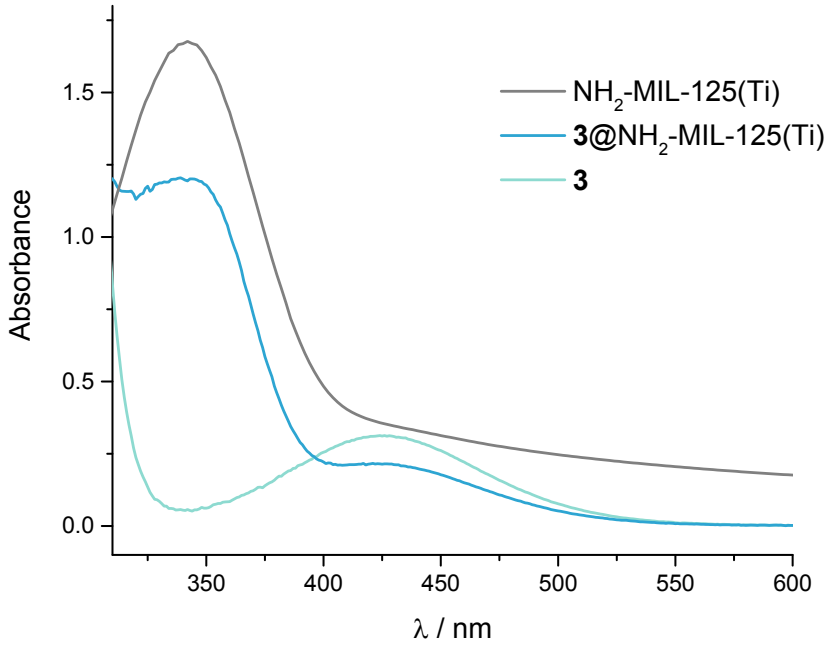

Figure S17. UV/VIS spectra of NH_2-MIL-125(Ti) (*grey*), **3**@NH_2-MIL-125(Ti) (blue) and **3** (light blue) in water.

12. Spectroelectrochemistry (SEC)

Spectroelectrochemistry experiments comprised the recording of the sample absorption spectra (ploted as ΔOD) upon the application of positive (leading to sample oxidation) or negative potentials (leading to sample reduction). The optical setup comprised a Deuterium-Halogen lamp DH-2000 as light source, a USB2000 UV-VIS Spectrometer and a NIRQUEST NIR spectrometer (all from Ocean Optics). The potential was applied by an Analyser CHI832B from CH Instruments. For the measurements, a quartz cell was used. This cell included a platinum CE and an Ag wire as pseudo-RE. Translucent plates of glass coated with indium tin oxide (ITO) were used as WE. $LiClO_4$ in acetonitrile (0.1 M) was used as electrolytes for the oxidation of **3**. All solutions were bubled through with argon to avoid the presence of oxygen.

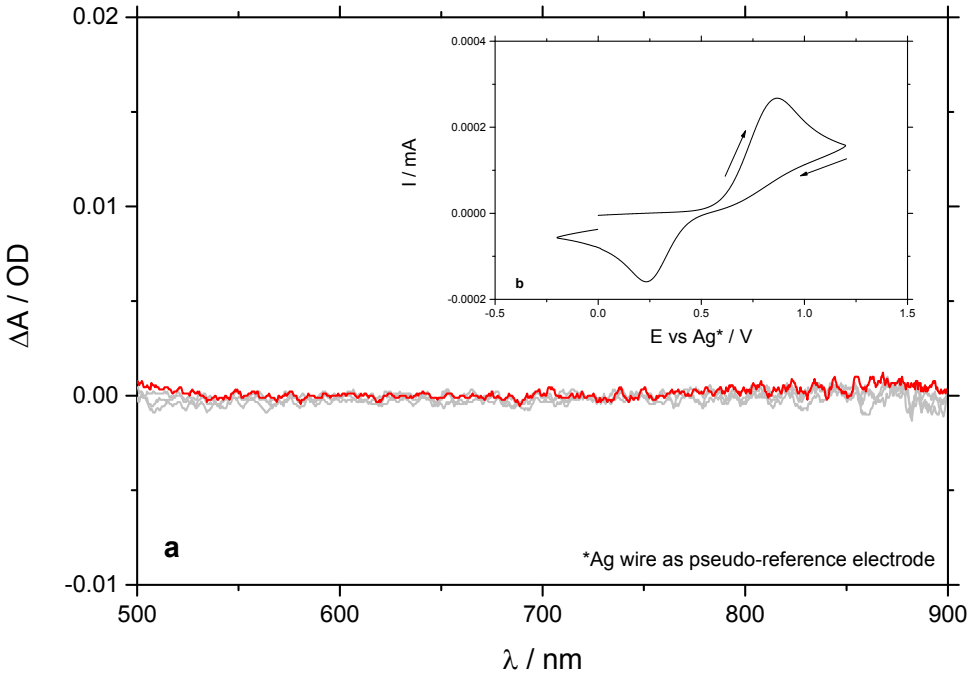

Figure S18. Absorption spectral changes of **3** (TEMPO) in acetonitrile ($1 \cdot 10^{-3}$ M) upon closure of the oxidation cycle. Inset (panel b) displays the registered cyclic voltammogram. Panel a shows that no change in absorbance was measured while applying positive bias. The arrows indicate the scan direction. The scan rate was 50 mV/s.

13. VIS-pump VIS-probe TEMPO

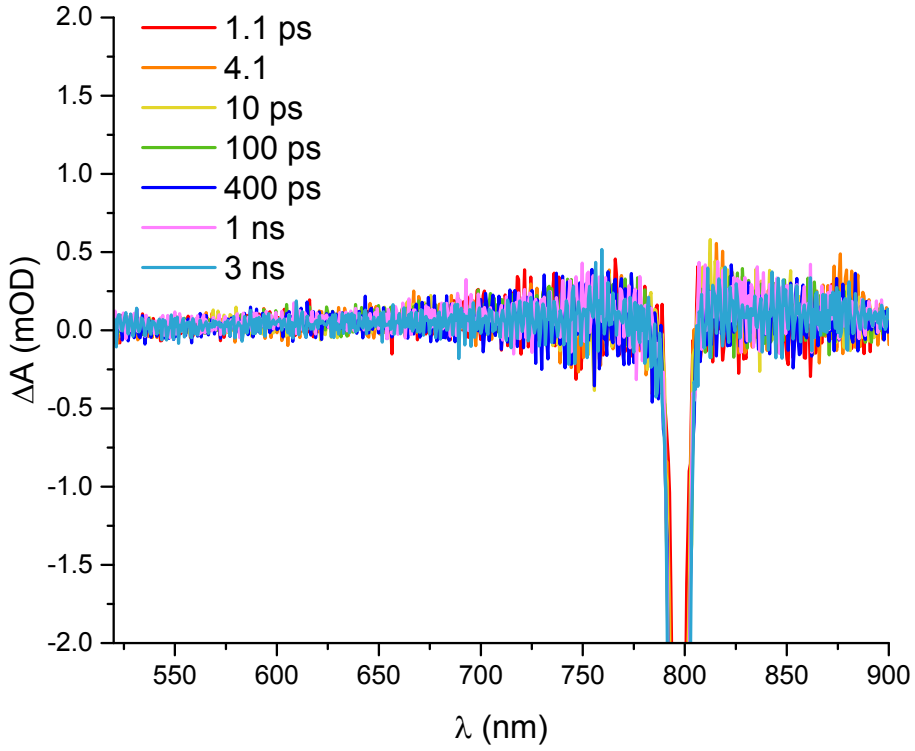

Figure S19. Differential transient absorption spectra for **3** in water upon excitation at 400 nm. No transient signal (only noise) is observed.

14. Reactivity

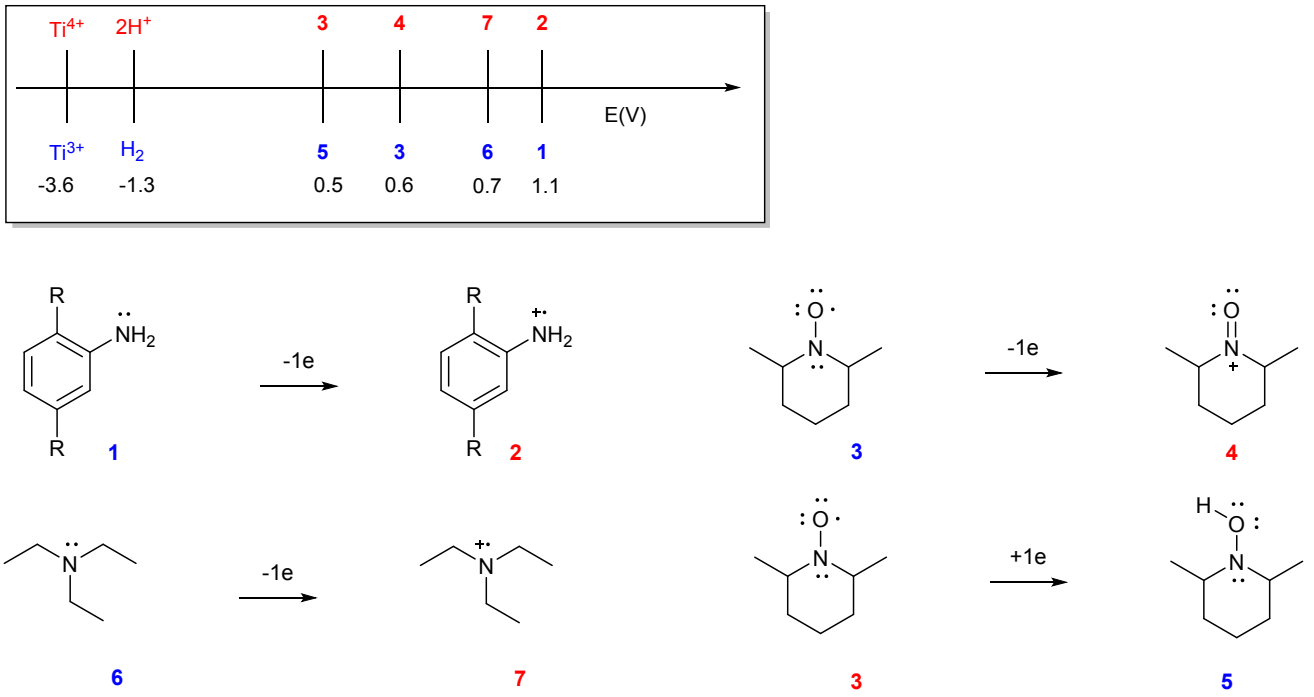

Figure S20. Scheme of the relative redox potentials of the compounds here studied (Top). Oxidation or reduction half reactions of compounds **1**, **2**, and **3**.

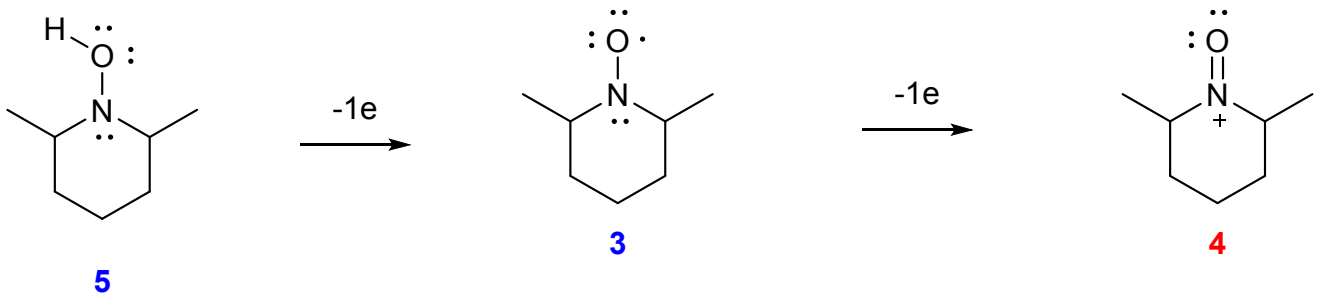

Figure S21. Reactivity of compound **3** (TEMPO). This indicates that either the one-electron oxidised **3** is reduced again via interaction with Ti^{3+}, or neutral **3** is directly reduced by Ti^{3+}. The proton source is water impurity from the solvent.

15. Photocatalytic hydrogen evolution

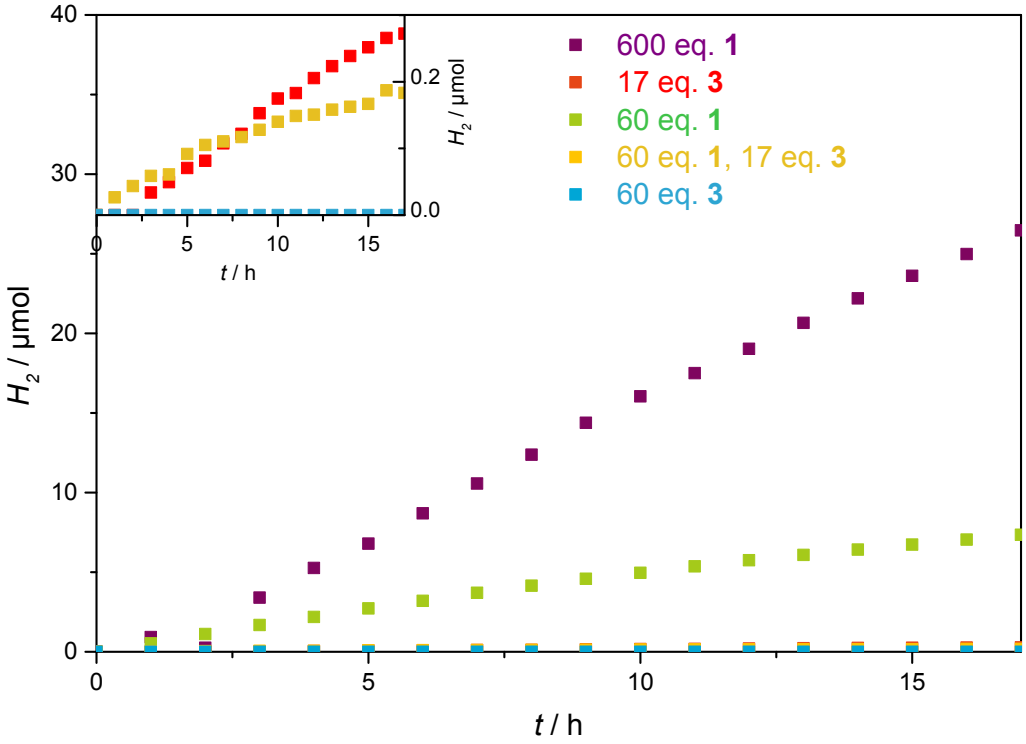

Figure S22. Photocatalytic hydrogen evolution under illumination at >385 nm light. 23.5 mL acetonitrile, 0.5 mL water, 30 mg NH_2-MIL-125 and 600 eq. (4.7 mL) **1** (*purple*), 17 eq. (150 mg) **3** (*red*), 60 eq. (0.5 mL) **1** (*green*), 60 eq. **1** and 17 eq. **3** (0.5 mL **1**+150 mg **3)** (*yellow*), and 60 eq. (500 mg) **3** (*blue*).

16. Photocatalytic benzaldehyde evolution

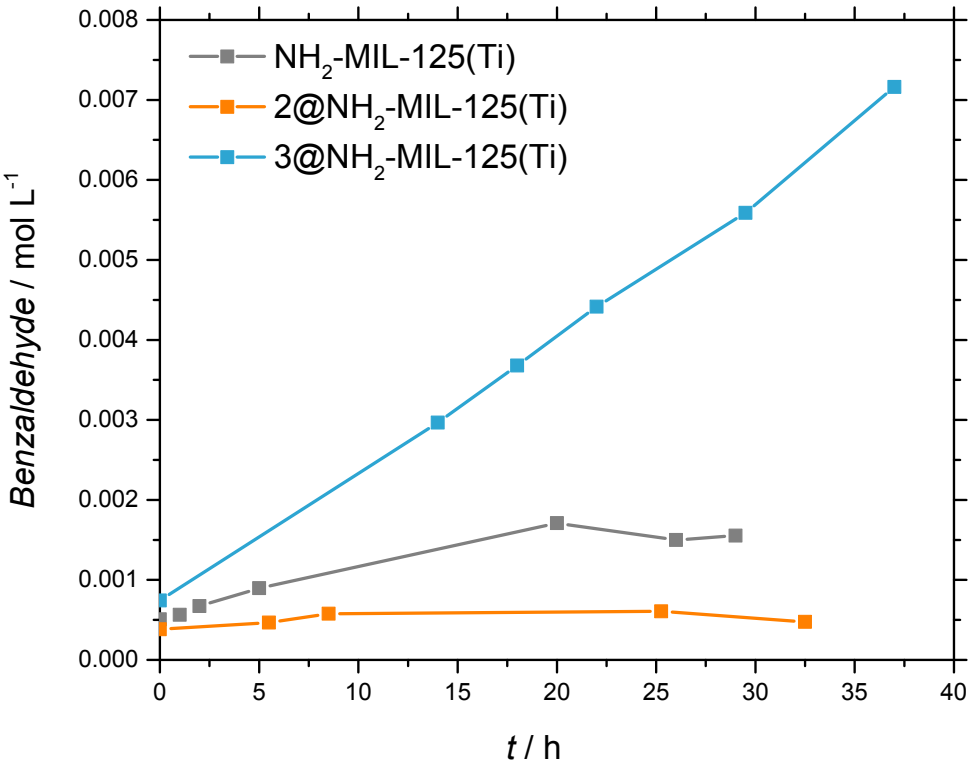

Figure S23. Photocatalytic benzaldehyde evolution. NH_2-MIL-125(Ti) (grey), **2**@NH_2-MIL-125(Ti) (orange) and **3**@NH_2-MIL-125(Ti) (blue). 35 mL acetonitrile, 0.31 mL 1,2-dichlorobenxene, 0.58 mL benzyl alcohol, 35 mg NH_2-MIL-125(Ti), 38 mg of **2** and 37 mg of **3**.

TEMPO has already been applied for oxidation catalysis. The oxoammonium cation $TEMPO^+$ (oxidized TEMPO) is a relatively strong oxidant (E^0=0.53V). For its application, an extra oxidant compound must be used (m-chloroperbenzoic acid, sodium bromite, sodium hypochlorite, among others) in order to apply TEMPO as co-catalyst.[6] The stoichiometric application of TEMPO as oxidant is only possible for systems with pH lower than 3, where TEMPO disproporcionates and the effective oxidant is produced without the aid of the additional oxidant. To probe the charge transfer from **3**@$N^{\bullet-}H_2$-MIL-125(Ti^{3+}) --> **3**$^{\bullet-}$@NH_2-MIL-125(Ti^{3+}), we performed catalytic oxidation tests using benzyl alcohol as substrate. The photo-oxidation activity using the pristine NH_2-MIL-125(Ti) as catalyst and O_2 as end oxidant is low. When using the **3**@NH_2-MIL-125(Ti) pair, the catalytic activity clearly increases. In contrast, when using **2**@NH_2-MIL-125(Ti), the catalytic activity is negligible.

[1] M. F. De Lange, T. J. H. Vlugt, J. Gascon, F. Kapteijn *Microporous and Mesoporous Materials*. **2014**, 200, 199-215.
[2] S. K. Bharti and R. Roy, TrAC Trends in Analytical Chemistry, **2012**, 35, 5-26.
[3] M. A. Nasalevich, R. Becker, E. V. Ramos-Fernandez, S. Castellanos, S. L. Veber, M. V. Fedin, F. Kapteijn, J. N. H. Reek, J. I. van der Vlugt, J. Gascon *Energy & Environmental Science*. **2015**.
[4] M. A. Nasalevich, C. H. Hendon, J. G. Santaclara, K. Svane, B. van der Linden, S. L. Veber, M. V. Fedin, A. J. Houtepen, M. A. van der Veen, F. Kapteijn, A. Walsh, J. Gascon *Scientific Reports*. **2016**, 6, 23676.
[5] J. G. Santaclara, M. A. Nasalevich, S. Castellanos, W. H. Evers, F. C. M. Spoor, K. Rock, L. D. A. Siebbeles, F. Kapteijn, F. Grozema, A. Houtepen, J. Gascon, J. Hunger, M. A. van der Veen *ChemSusChem*. **2016**, 9, 388-395.
[6] R. A. Sheldon, I. W. C. E. Arends *Advanced Synthesis & Catalysis*. **2004**, 346, 1051-1071.